

Testing competing hypotheses for soil magnetic susceptibility using a new chemical kinetic model

John F. Boyle^{1*}, John A. Dearing², Antony Blundell³, and Jacqueline A. Hannam⁴

¹Department of Geography, University of Liverpool, Liverpool L69 7ZT, UK

²School of Geography, University of Southampton, Southampton SO17 1BJ, UK

³School of Geography, University of Leeds, Leeds LS2 9JT, UK

⁴Natural Resources Department, National Soil Resources Institute, School of Applied Sciences, Cranfield University, Cranfield, MK43 0AL, UK

ABSTRACT

A chemical kinetic model is presented for the formation and accumulation of secondary ferrimagnetic minerals (SFMs) in soil constructed using experimentally determined rate constants and validated against field data. The primary objective is to critically assess the significance of competing causal mechanisms and disputed environmental controls under temperate conditions. Four findings are important in relation to current application of soil magnetic susceptibility data. First, transformation of hydrous ferric oxide to magnetite should dominate SFM formation, controlled primarily by parent material ferrous silicate concentration and climate. Second, abiotic reactions should account for most of the SFM production; the most significant impact of high Fe²⁺ concentrations created by dissimilatory iron-reducing bacteria is enhanced export of iron from the soil in runoff. Third, the model predicts a correlation between hematite and magnetite concentrations, weakening field support for direct transformation of hydrous ferric oxide to maghemite. Fourth, magnetic susceptibility enhancement should increase strongly with weathering duration.

INTRODUCTION

The formation of secondary ferrimagnetic minerals (SFMs) and their contribution to soil magnetic properties is important to a number of fields of geological and environmental research. Soil magnetic properties are widely used as climate proxies in loess-paleosol sequences (e.g., Kukla et al., 1988), “fingerprints” of sediment sources (e.g., Walling et al., 1979), records of atmospheric pollution (e.g., Oldfield et al., 1978), tools for archaeological mapping (e.g., Tite and Mullins, 1971), proxies for planetary atmospheric conditions (e.g., Barrón and Torrent, 2002), and an aid to detecting land mines (Hannam and Dearing, 2008). Despite this, mechanisms for SFM formation are disputed, beyond broad agreement that in free-draining temperate soils, Fe²⁺ released by dissolution of ferrous silicate is first oxidized to hydrous ferric oxide (HFO) and subsequently transformed to goethite, hematite, magnetite, and maghemite (Schwertmann, 1988). There are three principle schools of thought (Dearing et al., 1996; Blundell et al., 2009). First, Le Borgne (1955) and later Mullins (1977) proposed a “fermentation” process whereby wetting and drying cycles promote anaerobic bioreduction of Fe, and then precipitation of magnetite or maghemite particles. Second, Maher and Taylor (1988) showed that magnetite could form without dissimilatory Fe-reducing bacteria (DIRB), and suggested that soil magnetic enhancement involves competitive abiotic reactions (Maher, 1998). Third, Barrón et al. (2003) and Torrent et al. (2006) proposed that SFM formation is controlled by abiotic aging of HFO via maghemite to hematite, based on experimental evidence for the transient formation of hydromaghemite, now thought to be a ferrimagnetic form of ferrihydrite (Cabello et al., 2009). In addition, fire-induced magnetization was observed by Le Borgne (1960), but subsequent studies (Dearing et al., 1996) limit its role, at least in temperate environments.

In a study of soil magnetic susceptibility at ~5000 sites across England and Wales, Blundell et al. (2009) showed ~30% of variability to be

explained by parent material and drainage, with lesser roles for other factors, including mean annual precipitation. They concluded that three issues remain in question:

1. Which reaction pathways dominate pedogenic SFM formation? Opposing views (cf. Barrón and Torrent, 2002; Dearing et al., 1996) imply fundamentally different environmental controls.

2. What role does weathering duration play? Opposing views (cf. Maher, 1998; Vidic et al., 2004) affect our interpretation of loess paleo-precipitation records.

3. What role do DIRB play? If DIRB are important, then our current uncertainty about their abundance in soils hinders our understanding of soil magnetic enhancement.

These questions cannot be addressed using empirical evidence alone (Blundell et al., 2009), due to weak environmental correlations and problems quantifying potential drivers. Nor have laboratory data provided unambiguous answers (e.g., Hansel et al., 2005) owing to the difficulty of replicating soil environments at suitable time scales. Here we develop a quantitative process model that integrates different conceptual models with existing laboratory and field studies, allowing us to assess competing processes more critically. Published reaction kinetic data are combined in a predictive model that tests which reactions should be sufficiently rapid to have an impact on the pool of reaction products. Pivotal to this approach is estimation of the Fe²⁺ supply rate to soil from primary mineral weathering under differing environmental conditions, provided by the ALLOGEN model (Boyle, 2007; see the GSA Data Repository¹ for a description and discussion of reliability).

MODEL COMPONENTS AND FRAMEWORK

The choice of mineral reactions to include in the model must partially depend on availability of suitable chemical kinetics data (summarized in Table DR1 in the Data Repository). Transformation of magnetite to maghemite, though known to occur, is insufficiently quantified to include. As the two minerals have similar magnetic properties, we assume that our predicted χ_{lf} (low-frequency magnetic susceptibility) values are unaffected by complete or partial transformation. We also, for lack of suitable kinetic data, neglect possible direct formation of goethite from Fe²⁺ oxidation (e.g., Cornell and Schwertmann, 2003).

The chemical model assumes (e.g., Maher, 1998) that reactions proceed concurrently and competitively, applying them in a simple conceptual soil model that must address two issues. First, to allow for contrasting water:particle ratios between laboratory (water saturated) and field (lower and variable water content) conditions, rates and quantities for interacting dissolved and particulate species are expressed on a volumetric basis, with aqueous concentrations based on flux ratios. Second, Fe²⁺ will form HFO only under oxidizing conditions, while DIRB need anoxia to reduce HFO to Fe²⁺. For coexistence of aerobic and anaerobic conditions, we must separate these states in either space or time. We have chosen alterna-

¹GSA Data Repository item 2010291, methods, mineral reaction kinetic data, and data sources, is available online at www.geosociety.org/pubs/ft2010.htm, or on request from editing@geosociety.org or Documents Secretary, GSA, P.O. Box 9140, Boulder, CO 80301, USA.

*E-mail: jfb@liv.ac.uk.

tion with time, partly for computational simplicity, and partly because the analogy with wetting-drying cycles has synergies with the hypothesized mechanisms. Sensitivity tests show that cycle duration has little impact (set at 0.1 yr), while the oxic fraction (relative duration of the oxygenated subcycle) is important. The oxic fraction at 0.5 promotes optimal SFM formation; higher values favor goethite and hematite while lower values enhance runoff export of Fe^{2+} at the expense of all secondary iron phases. On the basis that soil pores are aerated if moisture is below field capacity but waterlogged if above, the oxic fraction is equated to the proportion of days that soil moisture is below field capacity.

Figure 1 illustrates the reactions included for each redox state. Ferromagnetic ferrihydrite (cf. Cabello et al., 2009) is excluded because the dependence of reaction rate on aqueous anion composition (which is unknown) during formation of HFO leaves the reaction kinetics inadequately constrained. We therefore test the significance of this pathway only indirectly by exploring whether the model yields significant SFM formation in its absence. Also neglected are anaerobic dissolution of magnetite, shown to occur in some slowly accumulating lake sediments (Snowball, 1993) and waterlogged gley soils (Dearing et al., 1996; Blundell et al., 2009), but which is rare in freely drained soils, and bacterial magnetosomes, which generally make only a very minor contribution to soil SFM content (Dearing et al., 2001).

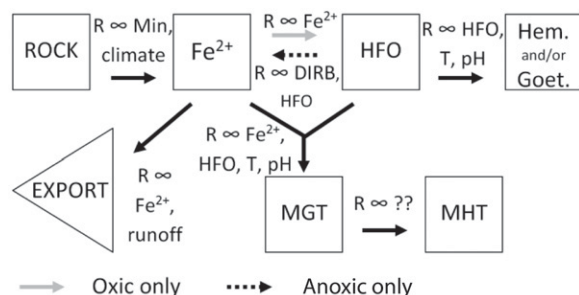


Figure 1. Simplified scheme for competitive production of magnetite (MGT), maghemite (MHT), and goethite (Goet.) and/or hematite (Hem.) from hydrous ferric oxides (HFO, e.g., ferrihydrite) through cycles of oxidizing and reducing conditions in the presence of dissimilatory iron reducing bacteria (DIRB). T—temperature, Min—minerals.

The model is coded using Microsoft® Visual Basic for Applications in Excel. Separate procedures implement ALLOGEN silicate dissolution rate calculations (giving the Fe^{2+} supply rate), competitive iron mineral transformation, and other data handling. The reactions are addressed by solving the mass-balance conditions for Fe^{2+} activity:

$$\text{Oxic: } R(\text{Fe}^{2+} \text{ supply}) = R(\text{Fe}^{2+} \text{ runoff export}) + R(\text{Fe}^{2+} \rightarrow \text{HFO}) + R(\text{Fe}^{2+} + \text{HFO} \rightarrow \text{magnetite})$$

$$\text{Anoxic: } R(\text{Fe}^{2+} \text{ supply}) + R(\text{DIRB, HFO} \rightarrow \text{Fe}^{2+}) = R(\text{Fe}^{2+} \text{ runoff export}) + R(\text{Fe}^{2+} + \text{HFO} \rightarrow \text{magnetite}),$$

where each term is a rate expression (Table DR1) for reactions generating or consuming Fe^{2+} . Solving for Fe^{2+} activity allows calculation of mineral formation rates and primary mineral depletion by weathering, and tracking of mineral accumulation through time. (For conversion of SFM concentration to χ_{lf} , see the Data Repository.)

RESULTS AND DISCUSSION

By running the model under a range of conditions (e.g., climate, parent material) we explore factors influencing the expected final mix of soil iron phases.

Main Environmental Factors

The strongest environmental factor is parent material ferrous silicate concentration (Fig. 2), which affects both the quantity and type of secondary iron minerals via control over the supply rate of Fe^{2+} (linearly related to the chlorite concentration; 2.0×10^{-12} moles $\text{L}^{-1} \text{ s}^{-1}$ at 50 wt% for this model run). Hematite and goethite increase linearly with primary silicate concentration, while magnetite increases quadratically due to concurrent enhancement of HFO and dissolved Fe^{2+} , its formation rate depending on both. Increasing the mean annual precipitation (MAP), or to a lesser extent mean annual temperature (MAT), initially increases the concentration of all three minerals owing to enhancement of primary mineral weathering (Boyle, 2007). However, further increases inhibit magnetite formation as the oxic fraction falls with increasing MAP but increases with MAT.

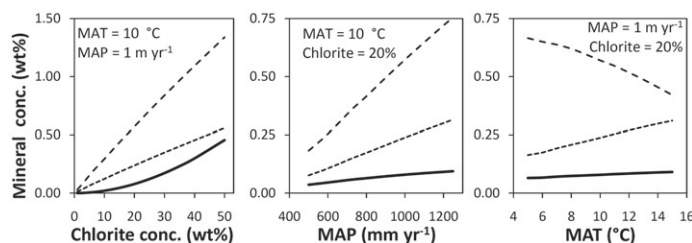


Figure 2. Environmental controls on modeled secondary magnetite (solid line), goethite (long dash), and hematite (short dash) after 10 k.y. of weathering. Oxic fraction is set at 0.5. MAT—mean annual temperature; MAP—mean annual precipitation; conc.—concentration.

Model Comparison with Soil Data

There are no published mineralogical data for most (75%) of the rock classes considered in Blundell et al. (2009). However, for some argillaceous rock types (Table DR1) there are sufficient mineral data to allow simulation of SFMs and comparison with observed soil χ_{lf} values (Blundell et al., 2009). The resulting predictions are highly correlated ($R^2 = 0.95$) with the observed data (Fig. 3A). The model is also applied (Fig. 3B) to the soil data set of Maher and Thompson (1995) using four different primary mineral concentrations, the site parent materials being unknown. The pattern of climatic dependence for χ_{lf} is well captured. These two comparisons suggest that our modeling framework for applying the experimentally determined rate constants generates realistic outcomes, but it is also clear

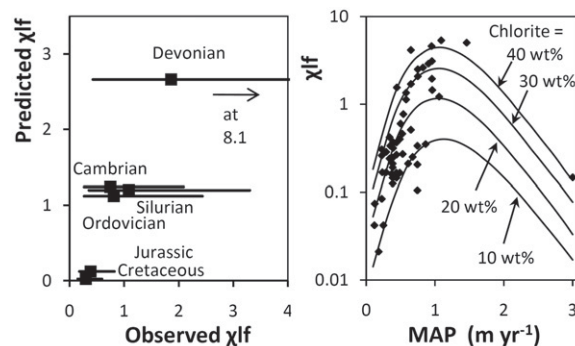


Figure 3. Predicted and observed soil χ_{lf} ($10^{-6} \text{ m}^3 \text{ kg}^{-1}$). A: UK soils on argillaceous rock categories. Observed χ_{lf} values are from England and Wales (Blundell et al., 2009). Simulation assumes 10 k.y. soil development under modern climate of each site. B: Symbols: Northern Hemisphere sites of Maher and Thompson (1995). Curves: Simulated values for 10, 20, 30, and 40 wt% chlorite (site values being unknown). Other parameters are listed in Data Repository (see footnote 1). MAP—mean annual precipitation.

that measured soil χ_{lf} values on any one parent material vary widely across sites. This is expected, as the rate of magnetite formation is sensitive to both MAP and parent material composition (Fig. 2A); interpolated meteorological data yield reasonable values for MAP, but the site mineral concentrations are estimated only from limited rock type means. Variable substrate composition is likely to be a major cause of wide scatter in observed χ_{lf} values for soil survey samples (Blundell et al., 2009).

Role of Ferrimagnetic Ferrihydrite

Cabello et al. (2009) stated that in the absence of primary magnetite, ferrimagnetic ferrihydrite formed by oxidative transformation of HFO could explain soil magnetic enhancement, evidence interpreted by Torrent et al. (2010) to support the existence of a direct pathway from HFO to maghemite. Direct evidence for this is lacking: ferrimagnetic ferrihydrite has not been reported in soils and the published rate data are few. Cabello et al. (2009) stated that their ferrimagnetic ferrihydrite pathway is proven by the widely observed correlation of χ_{lf} with hematite in soils. Our results contradict this; a correlation of magnetite and hematite (Fig. 4) arises simply from concurrent formation. Furthermore, we find satisfactory prediction of χ_{lf} (e.g., Fig. 3) despite neglecting the pathway.

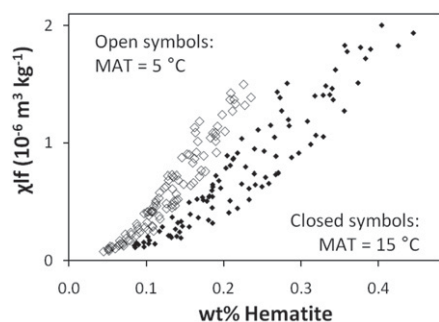


Figure 4. Correlation of modeled χ_{lf} and hematite concentration at mean annual temperature (MAT) = 5 and 15 °C; parent material chlorite concentration and local mean annual precipitation varied randomly within fixed limits.

Role of DIRB

Laboratory experiments show that DIRB can reduce HFO under anoxic conditions, and that Fe^{2+} released can react with excess HFO to form magnetite (e.g., Bonneville et al., 2004). Our model permits prediction of HFO and Fe^{2+} concentrations from Fe supply rate and DIRB cell density, but the lack of cell density data precludes direct evaluation. Instead, we can explore the influence of DIRB density on Fe cycling and magnetite formation. Figure 5 compares model runs at cell densities of 10^8 and 10^{10} cells L^{-1} , values that separate differing model behavior. At a cell density of 10^8 or lower, Fe^{2+} supply from bacterial reduction is low compared with primary Fe^{2+} release. At densities $>10^{10}$, bacterial reduction rapidly increases Fe^{2+} at the expense of HFO, initially enhancing magnetite formation but then decreasing it as HFO depletion becomes limiting. However, DIRB can positively affect magnetite formation if anoxic episodes are brief relative to oxic conditions; the transient enrichment of both HFO and Fe^{2+} upon deoxygenation favors magnetite. However, the amount of magnetite formed under such conditions is never greater than would occur at 0.5 oxic fraction without DIRB. Thus magnetite production depends upon HFO and Fe^{2+} together, both of which are supplied ultimately by the primary silicate dissolution. For any given primary Fe supply rate, there is a single optimum magnetite production rate, achieved when HFO and Fe^{2+} activities are balanced. If primary Fe release is all Fe^{2+} , this optimum occurs with DIRB $<10^8$ and 0.5 oxic fraction. At higher oxic fractions, DIRB have a greater role to play in achieving the optimum; but, even where all primary Fe is released as Fe^{3+} , and thus DIRB are essential for magnetite formation, the maximum amount is still accurately predicted by the optimal abiotic case.

The observation that DIRB are not essential for optimal formation of secondary magnetite does not contradict the established causal link between

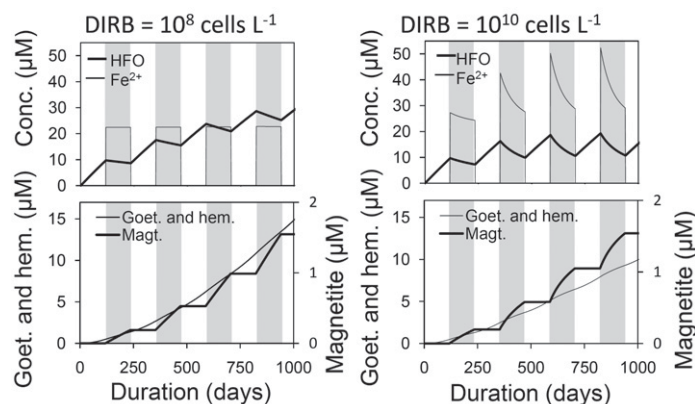


Figure 5. Accumulation of hydrous ferric oxide (HFO), magnetite (Magt.), and goethite (Goet.) and/or hematite (hem.) through time under two different dissimilatory iron-reducing bacteria (DIRB) cell densities and simple alternation of oxic and anoxic periods. Mean annual temperature = 9 °C, mean annual precipitation = 1 m yr^{-1} , primary Fe supply rate = 1×10^{-12} moles $L^{-1} s^{-1}$. Cycle length increased to 240 days to better illustrate curve shape. Stripes show oxic state; gray indicates anoxia; Conc.—concentration.

DIRB activity and episodic Fe^{2+} enhancement in soil solutions. We suggest simply that such episodes need not contribute greatly to SFM formation, and can be ignored when calculating their expected maximum concentrations.

Role of Time

The relationship between modeled soil χ_{lf} and weathering duration (Fig. 6A) shows two stages in the temporal development of magnetic enhancement. The first stage involves active production of SFMs from Fe^{2+} released by primary minerals (e.g., chlorite). Initially rapid, the rate of increase declines as weathering depletes the parent mineral (half-life in soil $\approx 10^4$ yr) limiting the duration of this effect to $\sim 10^5$ yr. The second stage involves passive enhancement of SFM concentration due to loss of other, less reactive, minerals from the soil by weathering (e.g., feldspars). This acts far more slowly, with a characteristic time of $\sim 10^5$ yr. The rates for the two stages will vary with mineralogy and climate, but should both occur where time permits. Vidic et al. (2004) presented data for dependence of χ_{lf} on particle residence times in Chinese loess (residence time is used rather than soil age owing to the high rate of accretion, but the principle is identical). The similarity between modeled and observed values (Fig. 6B) offers support for the active stage predicted by

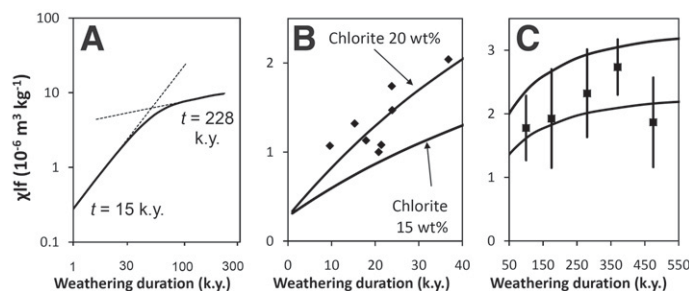


Figure 6. Time-dependent changes in χ_{lf} . A: Two-stage temporal development of χ_{lf} ; t —time. B: Symbols: Chinese loess data (means after Vidic et al., 2004). Lines: Model output for mean annual precipitation = 600 mm/yr, chlorite concentration 15 and 20 wt%. C: Symbols: Data for the Santa Cruz (California) marine terrace chronosequence (E. Ciclitira, J. Clear, and E. Perrin, 2010, personal commun.). Lines: Model output based on 3 wt% hornblende and 8 wt% biotite, mean modern climate, and 0.1 and 0.2 wt% initial inherited magnetite. Mineral data sources are provided in the Data Repository (see footnote 1).

our model. To test the passive stage, we turn to evidence on a far longer time scale. Singer et al. (1992) reported a limited data set showing time dependence for the ~500 k.y. marine terrace soil chronosequence at Santa Cruz, California. A new, fuller, data set for this chronosequence (Fig. 6C) shows reasonable agreement with the model output.

Future Modeling Needs

Overall, the model outputs show good agreement with observed data, and with wider testing there is the potential to produce a general predictive model for magnetic properties in different soil types. At present, general application is hindered by three areas of uncertainty. First, using the field capacity concept to estimate the oxic fraction model parameter is inadequately tested. This is relatively unimportant for well-drained temperate soils, but is potentially an issue at soil moisture extremes. Second, though DIRB are found to be of secondary importance to a generalized model, our ignorance of their natural concentrations leaves room for doubt about their significance in specific cases. Third, and most significant, global maps of bedrock mineral composition are needed for reliable prediction of pedogenic SFM formation. Furthermore, the sensitivity of SFM formation to the substrate ferrous silicate concentration is such that generalized rock-type mineralogical data would be insufficient for accurate prediction at specific sites.

CONCLUSIONS

Using only experimentally determined rate constants and measured parent material concentrations of primary Fe silicate minerals, the model prediction of SFM concentration agrees with field-observed average values for well-drained temperate soils. The model predicts that the main controlling variables are the primary ferrous silicate concentration and MAP, with a lesser role for MAT. The importance of primary mineral concentration, variable and poorly quantified for most parent materials, is a significant barrier to prediction of soil magnetic susceptibility enhancement at global, regional, and field scales.

Abiotic dissolution of ferrous silicates provides a sufficient flux of Fe^{2+} to allow coexistence of hydrous ferric oxide and aqueous Fe^{2+} (via alternation of redox states) at high enough concentrations to form SFMs. Though DIRB can contribute to magnetite formation, excessively high DIRB concentrations discourage magnetite formation by allowing secondary iron to leak from the soil.

The model predicts a correlation between SFMs and hematite even in the absence of a $\text{HFO} \rightarrow \text{maghemite} \rightarrow \text{hematite}$ pathway. Consequently, such a correlation offers no support for the existence of this pathway, with potentially wide-ranging implications, for example, in terms of interpreting past environmental conditions on Earth and Mars (cf. Barrón and Torrent, 2002).

The model predicts a strong time dependence for soil magnetic susceptibility enhancement, occurring in two stages caused by different mechanisms acting at different temporal scales (characteristic times $\sim 10^4$ and 10^5 yr). Thus, care should be exercised in interpreting χ_{lf} values used to monitor long-term change ($>10^3$ yr), such as reconstruction of catchment sediment sources from lake sediment records. The model provides a plausible basis for estimating the weathering duration impact when interpreting paleosol magnetism.

ACKNOWLEDGMENTS

This research was supported by Natural Environment Research Council–Defence Science and Technology Laboratory grant NE/D000963/2.

REFERENCES CITED

Barrón, V., and Torrent, J., 2002, Evidence for a simple pathway to maghemite in Earth and Mars soil: *Geochimica et Cosmochimica Acta*, v. 66, p. 2801–2806, doi: 10.1016/S0016-7037(02)00876-1.

Barrón, V., Torrent, J., and de Grave E., 2003, Hydromaghemite, an intermediate in the hydrothermal transformation of 2-line ferrihydrite into hematite: *American Mineralogist*, v. 88, p. 1679–1688.

Blundell, A., Dearing, J.A., Boyle, J.F., and Hannam, J.A., 2009, Controlling factors for the spatial variability of soil magnetic susceptibility across England and Wales: *Earth-Science Reviews*, v. 95, p. 158–188, doi: 10.1016/j.earscirev.2009.05.001.

Bonneville, S., van Cappellen, P., and Behrends, T., 2004, Microbial reduction of iron(III) oxyhydroxides: Effects of mineral solubility and availability: *Chemical Geology*, v. 212, p. 255–268, doi: 10.1016/j.chemgeo.2004.08.015.

Boyle, J.F., 2007, Simulating loss of primary silicate minerals from soil due to long-term weathering using ALLOGEN: Comparison with soil chronosequence, lake sediment and river solute flux data: *Geomorphology*, v. 83, p. 121–135, doi: 10.1016/j.geomorph.2006.06.027.

Cabello, E., Morales, M.P., Serna, C.J., Barrón, V., and Torrent, J., 2009, Magnetic enhancement during the crystallization of ferrihydrite at 25 and 50°C: *Clays and Clay Minerals*, v. 57, p. 46–53, doi: 10.1346/CCMN.2009.0570105.

Cornell, R.M., and Schwertmann, U., 2003, *The iron oxides: Structure, properties, reactions, occurrences and uses* (second edition): Weinheim, Wiley VCH, 667 p.

Dearing, J.A., Hay, K., Baban, S., Huddleston, A.S., Wellington, E.M.H., and Loveland, P.J., 1996, Magnetic susceptibility of topsoils: A test of conflicting theories using a national database: *Geophysical Journal International*, v. 127, p. 728–734, doi: 10.1111/j.1365-246X.1996.tb04051.x.

Dearing, J.A., Hannam, J.A., Anderson, A.S., and Wellington, E.M.H., 2001, Magnetic, geochemical and DNA properties of highly magnetic soils in England: *Geophysical Journal International*, v. 144, p. 183–196, doi: 10.1046/j.0956-540X.2000.01312.x.

Hannam, J.A., and Dearing, J.A., 2008, Mapping soil magnetic properties in Bosnia and Herzegovina for landmine clearance operations: *Earth and Planetary Science Letters*, v. 274, p. 285–294, doi: 10.1016/j.epsl.2008.05.006.

Hansel, C.M., Benner, S.G., and Fendorf, S., 2005, Competing Fe(II)-induced mineralization pathways of ferrihydrite: *Environmental Science & Technology*, v. 39, p. 7147–7153, doi: 10.1021/es050666z.

Kukla, G., Heller, F., Liu Xiu Ming, Xu Tong Chun, Liu Tung Sheng, and An Zhi Sheng, 1988, Pleistocene climates in China dated by magnetic susceptibility: *Geology*, v. 16, p. 811–814, doi: 10.1130/0091-7613(1988)016<0811:PCICDB>2.3.CO;2.

Le Borgne, E., 1955, Susceptibilité magnétique anormale du sol superficiel: *Annales de Geophysique*, v. 11, p. 399–419.

Le Borgne, E., 1960, Influence du feu sur les propriétés magnétique du sol et sur celles du schiste et du granit: *Annales de Geophysique*, v. 16, p. 159–195.

Maher, B.A., 1998, Magnetic properties of modern soils and Quaternary loessic paleosols: Paleoclimatic implications: *Palaeogeography, Palaeoclimatology, Palaeoecology*, v. 137, p. 25–54, doi: 10.1016/S0031-0182(97)00103-X.

Maher, B.A., and Taylor, R.M., 1988, Formation of ultra fine-grained magnetite in soils: *Nature*, v. 336, p. 368–370, doi: 10.1038/336368a0.

Maher, B.A., and Thompson, R., 1995, Paleorainfall reconstructions from pedogenic magnetic susceptibility variations in the Chinese loess and paleosols: *Quaternary Research*, v. 44, p. 383–391, doi: 10.1006/qres.1995.1083.

Mullins, C.E., 1977, Magnetic susceptibility of the soil and its significance in soil science: A review: *Journal of Soil Science*, v. 28, p. 223–246.

Oldfield, F., Thompson, R., and Barber, K.E., 1978, The changing atmospheric fall-out of magnetic particles recorded in recent ombrotrophic peat sections: *Science*, v. 199, p. 679–680, doi: 10.1126/science.199.4329.679-a.

Schwertmann, U., 1988, Occurrence and formation of iron oxides in various pedoenvironments, in Stuki, J.W., et al., eds., *Iron in soils and clay minerals*: Dordrecht, Reidel Publishing Co., p. 267–302.

Singer, M.J., Fine, P., Verosub, K.L., and Chadwick, O.A., 1992, Time dependence of magnetic susceptibility of soil chronosequences on the California coast: *Quaternary Research*, v. 37, p. 323–332, doi: 10.1016/0033-5894(92)90070-Y.

Snowball, I.F., 1993, Geochemical control of magnetite dissolution in subarctic lake sediments and the implications for environmental magnetism: *Journal of Quaternary Science*, v. 8, p. 339–346, doi: 10.1002/jqs.3390080405.

Torrent, J., Barrón, V., and Liu, Q., 2006, Magnetic enhancement is linked to and precedes hematite formation in aerobic soil: *Geophysical Research Letters*, v. 33, L02401, doi: 10.1029/2005GL024818.

Torrent, J., Liu, Q.S., and Barrón, V., 2010, Magnetic susceptibility changes in relation to pedogenesis in a Xeralf chronosequence in northwestern Spain: *European Journal of Soil Science*, v. 61, p. 161–173.

Tite, M.S., and Mullins, C.E., 1971, Enhancement of the magnetic susceptibility of soils on archaeological sites: *Archaeometry*, v. 13, p. 209–219.

Vidic, N.J., Singer, M.J., and Versosub, K.L., 2004, Duration dependence of magnetic susceptibility enhancement in the Chinese loess-paleosols of the past 620 ky: *Palaeogeography, Palaeoclimatology, Palaeoecology*, v. 211, p. 271–288, doi: 10.1016/j.palaeo.2004.05.012.

Walling, D.E., Peart, M.R., Oldfield, F., and Thompson, R., 1979, Suspended sediment sources identified by magnetic measurements: *Nature*, v. 281, p. 110–113, doi: 10.1038/281110a0.

Manuscript received 24 June 2010

Manuscript accepted 30 June 2010

Printed in USA